

# Carbon Monoxide Gas Sensor Based on Nanocrystalline SnO<sub>2</sub> Thin Film Grown on Al<sub>2</sub>O<sub>3</sub> Substrate

**Amirhosein Asilian**  
Department of Electrical Engineering,  
Najafabad Branch,  
Islamic Azad University,  
Najafabad, Iran  
[ah.asilian@sel.iaun.ac.ir](mailto:ah.asilian@sel.iaun.ac.ir)

**S. Mohammadali Zanjani\***  
Smart Microgrid Research Center,  
Najafabad Branch,  
Islamic Azad University,  
Najafabad, Iran.  
[sma\\_zanjani@iaun.ac.ir](mailto:sma_zanjani@iaun.ac.ir)

**Reza Pournajaf**  
Advanced Materials Research Center,  
Najafabad Branch,  
Islamic Azad University, Najafabad,  
Isfahan, Iran  
[r.pournajaf@smt.iaun.ac.ir](mailto:r.pournajaf@smt.iaun.ac.ir)

**Reza Ebrahimi-kahrizangi**  
Advanced Materials Research Cer  
Najafabad Branch,  
Islamic Azad University, Najafab  
Isfahan, Iran  
[rezaebrahimi@pel.iaun.ac.ir](mailto:rezaebrahimi@pel.iaun.ac.ir)

## Abstract

This study addresses the imperative for advanced gas sensors, particularly for monitoring hazardous carbon monoxide (CO), by enhancing nanocrystalline SnO<sub>2</sub> thin film fabrication. Control of parameters in the sol-gel synthesis process is systematically explored to mitigate crack formation and enhance SnO<sub>2</sub> film quality on uncoated Al<sub>2</sub>O<sub>3</sub> substrates. Leveraging SnO<sub>2</sub>'s n-type semiconductor properties, traditional thin film methods are employed, with a specific focus on overcoming drawbacks through glycerin. Among various fabrication techniques, sol-gel proves cost-effective for producing high-quality, crack-free SnO<sub>2</sub> layers tailored for gas sensor applications. The study evaluates sensitivity to CO gas concentrations, improving structural integrity, sensitivity, and stability. X-ray powder diffraction and SEM imaging confirm phase purity and surface morphology, ensuring the absence of impurities or cracks. Integrated with microcontroller-based circuits, the sensors exhibit rapid response and recovery times crucial for real-time gas sensing. Adding an output circuit with enhanced resolution and stability further enhances sensor performance. Results demonstrate the proposed sensor's capability for rapid response (less than 30 seconds) and recovery times (~39 seconds), crucial for real-time gas sensing. Notably, the sensors demonstrate an admirable sensitivity with a minimum detection limit of as low as 1 ppm of CO gas. Additionally, the study validates the sensor's stability and reliability during prolonged exposure to N<sub>2</sub> and 1% CO mixtures, highlighting its potential for personal safety detectors and environmental safety monitoring.

**Keywords:** Nanocrystalline SnO<sub>2</sub>, Surface Morphology, Sol-Gel Synthesis, Readout Circuit, Environmental Monitoring.

## 1 Introduction

Tin oxide (SnO<sub>2</sub>) has garnered significant interest for a wide range of applications, including the detection of flammable gases, volatile organic compounds, and toxic gases, owing to its distinctive physical and chemical properties. SnO<sub>2</sub> is categorized as an n-type semiconductor, characterized by its tetragonal rutile structure and a substantial energy band gap of 3.6 eV at 300°K [1]. The synthesis of tin oxide (SnO<sub>2</sub>) nanoparticles in nanoscale dimensions and the form of coated layers have been carried out using various methods. It should be noted that the properties of these materials are highly dependent on particle size and

morphology. These parameters can be controlled by employing different synthesis techniques, which ultimately affect the sensitivity of tin oxide as a gas detection sensor. The primary methods used to produce SnO<sub>2</sub> nanoparticles and thin films include hydrothermal [2], sol-gel [3], and chemical vapor deposition techniques. In the study by Fan et al. [4], a nanosheet structure of SnO<sub>2</sub> was synthesized using a hydrothermal method with tin chloride hydrate and thiourea as raw materials. In Selvam et al.'s [5] research, thin-film SnO<sub>2</sub> coatings on glass substrates were synthesized using homogeneous precipitation and sol-gel dip-coating methods. Their results demonstrated a significant effect of multilayer SnO<sub>2</sub> coatings on sensing performance, with three-layered SnO<sub>2</sub> samples showing particularly high sensitivity.

The electrical resistance of tin oxide changes after the adsorption of various gas molecules, which enables its use as a sensor [6]. Consequently, sensitivity can be modified through different methods, including metal modifications with elements like palladium and platinum, compositing with metal oxides, and doping [7]. In a study by Simões et al. [8], SnO<sub>2</sub> nanoparticles were modified using palladium nanoparticles. The electrical characteristics showed that modifying SnO<sub>2</sub> nanoparticles with palladium altered their resistance at lower concentrations of CO gas dissolved in mineral oil, indicating potential applications in real-time monitoring of transformers. Additionally, Suvarna et al. [9] investigated antimony-doped SnO<sub>2</sub> (Sb-doped SnO<sub>2</sub>) as a highly precise sensor for detecting formaldehyde (HCHO) gas. Pure SnO<sub>2</sub> and Sb-doped SnO<sub>2</sub> nanostructures were prepared using the sol-gel method, resulting in improved structural and morphological properties.

On the other hand, carbon monoxide (CO) is a gas of paramount importance for monitoring due to its widespread occurrence in numerous contexts, such as residential heating systems, industrial operations, and emissions from vehicles. CO is notable for its lack of color and odor, and in elevated concentrations, it can pose a severe health risk [10]. Detecting CO is indispensable for safeguarding both industrial workplaces and the environment. Employing CO gas sensors represents a standard practice for issuing timely alerts about the accumulation of CO, effectively mitigating the potential for accidents and health-related dangers [11–13]. Lately, there has been ongoing research into the gas-sensing mechanism of SnO<sub>2</sub> films [14]. Typically, these gas sensing assessments have been conducted under elevated operating temperatures [15], which, in turn, have led to an extension in both response and recovery times.

To overcome the inherent deficiencies observed in various gas sensors, it's not unusual to employ a concoction of different oxides coupled with various additives. Using a composite of SnO<sub>2</sub> and Al<sub>2</sub>O<sub>3</sub> as a prime example, the Al<sub>2</sub>O<sub>3</sub> acts as a stabilizing agent, inhibiting the coalescence and expansion of SnO<sub>2</sub> granules. The augmentation of sensor performance, in terms of both sensitivity and stability, is attainable through the strategic application of these additives or through selecting an optimal oxide matrix. The infusion of assorted additives into metal oxides grants the ability to fine-tune an array of characteristics, including the concentration of charge carriers, the surface potential, barriers between grains, the phases within the composition, and even the granularity of particles. Such modifications to the chemical and structural properties of the metal-oxide gas sensors through judicious additive selection can significantly elevate their gas detection efficacy. Despite this, the definitive influence of various additives, whether they are oxides or other elemental forms, on the features of metal oxides remains largely enigmatic, propelling many in the research community to adopt a heuristic approach to these explorations. It is also noteworthy that extraneous impurities that cannot be regulated invariably impact the sensitivity of metal-oxide-based sensors [16].

It is clear that in gas detection technology, a diverse set of methods interact. However, the electrochemical approach is often not given the recognition it deserves. This efficiency is of particular import when it comes to the deployment of electrochemical sensors within handheld safety apparatuses tasked with the surveillance of harmful gases such as carbon monoxide (CO), oxygen (O<sub>2</sub>), nitrogen dioxide (NO<sub>2</sub>), and hydrogen sulfide (H<sub>2</sub>S). These devices are critically important in toxic gas detection scenarios where minute electrical interference is paramount since they are capable of functioning within such constraints. The

operational principle of electrochemical sensors involves the redox transitions where the gas of interest either relinquishes or gains electrons. Oxidizing gases like  $\text{H}_2\text{S}$ ,  $\text{SO}_2$ , and  $\text{NO}$  result in the depletion of electrons on the semiconductor's surface thereby leading to the formation of obstructions due to oxygen adsorption at the granular borders, escalating the sensor's surface resistance ( $R_s$ ). In contrast, reductive gases discount the absorbed oxygen level, leaving surplus electrons on the surface, thereby mitigating the surface resistance [15].

It is clear that while in most reported prior works, the sensor circuit design has been separated from the output reading mechanisms, the advances in Micro-Electro-Mechanical Systems (MEMS) have successfully integrated these components into a cohesive unit. A study identified as [17] explores the creation of a comprehensive gas sensor system that includes a logarithmic inverter circuit aimed at normalizing the output voltage. Further literature [18] dissects the formulation of gas sensor oscillator circuits capable of converting voltage to frequency, thus achieving high resolutions in detection. A collection of studies has embarked on pioneering tactics dedicated to managing the heater's temperature within the sensor and the precise calibration of the sensor's output [19 -23].

Instrumentation amplifiers (IAs) are an important component in precision signal processing due to their high input impedance, low output impedance, and excellent noise rejection capabilities. In the context of gas sensor systems, the main role of IA is to amplify low-level signals from the gas sensor while minimizing noise and interference. The key features expected from IA for these applications are: i) work effectively in a wide range of input voltages and make it compatible with different types of sensors. ii) The gain can be easily adjusted according to the desired sensitivity of the sensor. This is important for calibrating the system to detect specific carbon monoxide concentration levels. iii) Ensure that the accuracy of the sensor signal is maintained by reducing the effect of noise and interference. iv) It is suitable for battery-operated devices or systems, and their energy efficiency is excellent [24].

The present research focuses on the fabrication of nanocrystal  $\text{SnO}_2$  thin films and evaluates their performance as CO gas sensors in different gas concentrations. The solution to the issue of cracking in the thin films of nanocrystalline  $\text{SnO}_2$  on uncoated  $\text{Al}_2\text{O}_3$  layers is addressed using the sol-gel method. Consequently, this approach facilitates the development of thin-layer gas sensors. Subsequently, the second section presents the suggested design and execution of the associated sensor. The outcomes obtained from employing the proposed chromatographic sensor and the output reading circuit are delineated in the third part. The fourth section provides an examination of the suggested instrumental amplifier (IA) and its anticipated features, along with a review of the proposed electronic amplifier circuit designed to amplify the output signal from the Wheatstone Bridge. The recapitulation of the accomplished work is deferred to the fifth section..

## 2. Experimentals

Tin chloride dihydrate, high-purity ethanol, and glycerin (all Sigma Aldrich) were used for sol preparation. The alumina substrate was annealed at  $1400^\circ\text{C}$  before coating. To prepare the solution, first 7 grams of tin chloride dihydrate were dissolved in 20 milliliters of ethanol, placing the mixture in a sealed flask and subjecting it to magnetic stirring for 2 hours. Once complete dissolution was achieved, glycerin ( $\text{C}_3\text{H}_8\text{O}_3$ ) was added to the solution at a ratio of 1:12 to prevent the cracking of the coating. The stirring process continued for 3 hours at a temperature of  $70^\circ\text{C}$ . After polishing the alumina substrate and thoroughly cleaning it with ethanol and acetone to eliminate any contamination, the substrate was subjected to a temperature of  $90^\circ\text{C}$  to facilitate the evaporation of any remaining substances [25, 26]. Subsequently, following the printing of gold electrodes and a further cleaning step, the substrate was immersed in the gel cell solution within a dip-coating machine, where it remained at a constant speed for 3 seconds. After withdrawal from the solution, the substrate was placed in an oven set at a temperature of  $50^\circ\text{C}$  to allow the solvent to evaporate gradually. This process of applying the sensor coating was repeated 10 times in

preparation for X-ray powder diffraction (XRD) testing and characterization. Once the coated pieces had dried completely, they were put into an electric furnace for calcination, initiating the formation of  $\text{SnO}_2$ . This process was carried out at a heating rate of  $5\text{ }^\circ\text{C}$  per minute for 100 minutes. By incorporating the printing of two electrodes, each with a thickness of 0.8 micrometers, and applying an ENIG (Electroless nickel immersion gold) coating with a separation distance of 3.0 millimeters between each adjacent branch and a width of 254.0 micrometers for each branch, the sensor depicted in Figure 1-a was successfully produced.

The surface morphology of both the substrate and the coated sample was scrutinized utilizing a scanning electron microscope (SEM) (LEO 435VP). For XRD analysis of the initial powders, a Philips Xpert instrument was employed, operating at a voltage of 40 kV and a current of 30 mA. Furthermore, a copper cathode lamp with a wavelength of 1.54059 angstroms was utilized in this process. Figure 1-b shows the designed heater view. The sensor view before and after coating can be seen in Figure 1-a and Figure 1-c.

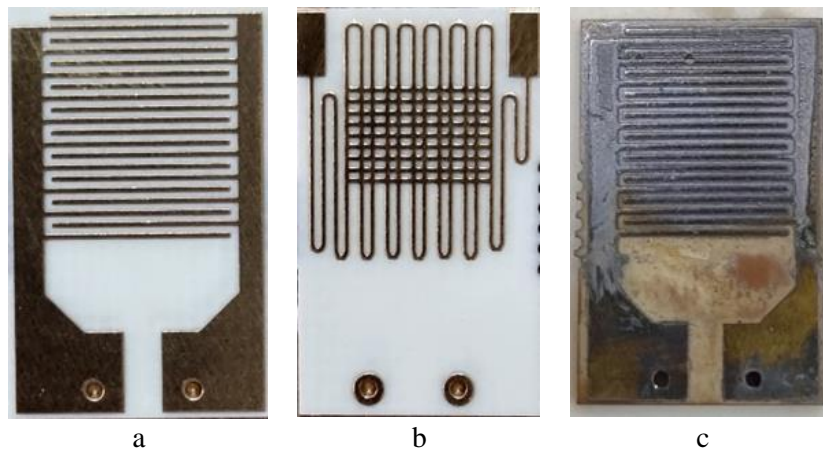


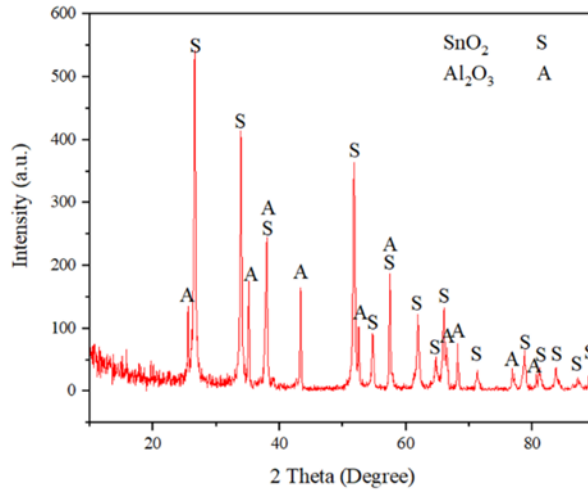
**Figure 1:** a) Sensor view before coating. b) Designed heater view. c) Sensor view after coating.

### 3. Results and discussion

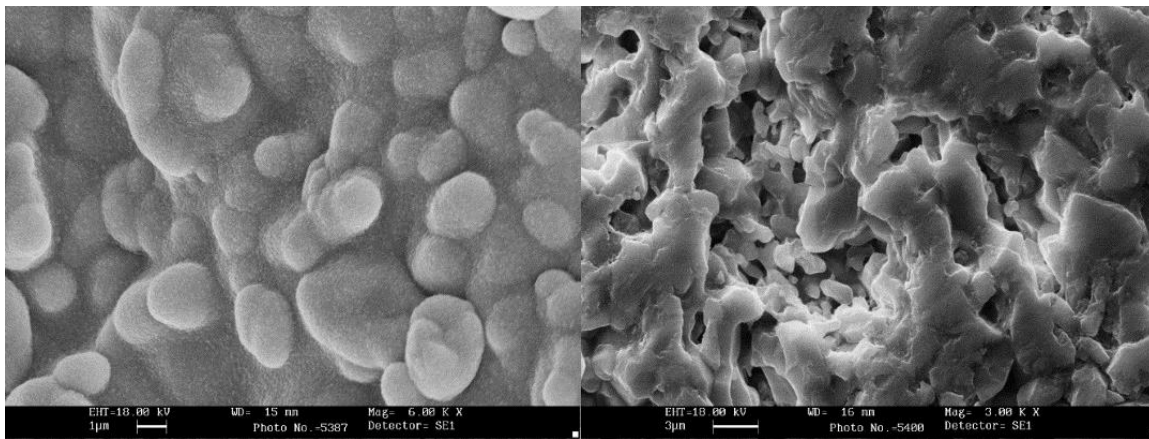
Figure 2 shows the X-ray diffraction pattern of the alumina sample coated with tin oxide. The peaks observed at  $2\theta$  of 48.26, 74.33, 56.51, and 80.37 correspond to the (110), (101), (211), and (200) planes of tin oxide with the reference card (JCPDS. no. 01-077-0448). The calculated crystalline size of the tin oxide phase using the Williamson-Hall [27] was approximately 26 nanometers. The peaks observed at  $2\theta$  of 13.35, 33.43, 47.57, and 56.25 correspond to the most intense peaks of the (104), (113), (116), and (012) planes of aluminum oxide with the reference card (JCPDS. no. 01-088-0826), respectively. The XRD pattern confirms the formation of a nanocrystalline tin oxide coating on the aluminum oxide substrate.

Figure 3 represents microscopic images of both the aluminum oxide substrate and the tin oxide-coated sample. Remarkably, the substrate displays no distinctive surface porosity. However, upon the coating, significant changes in surface morphology become evident. Although the porosity of the coating has increased significantly, no observable longitudinal or continuous cracks appear on the coated surface. Porosities play an important role in the performance of gas sensors, as they can profoundly influence the analytical response of the sensor. Higher porosity increases the activated surface area, thereby promoting greater adhesion of the target analyte to absorption pores, potentially affecting sensor accuracy [28, 29].

The thin tin oxide layer shows a uniform morphology and a nearly even distribution across the sample surface, with various sizes ranging below a micron.



**Figure 2:** XRD pattern of the coated aluminum sample.



**Figure 3:** Microscopic Images: a) Aluminum oxide substrate (left). b) SnO<sub>2</sub>-coated sample (right).

The cross-section of the alumina substrate coated with nanostructured tin oxide is shown in Figure 4. As can be seen in the figure, a layer with a thickness of about 1 micrometer is formed on the alumina substrate. According to the corresponding X-ray diffraction pattern, this layer contained only nanostructured tin oxide.

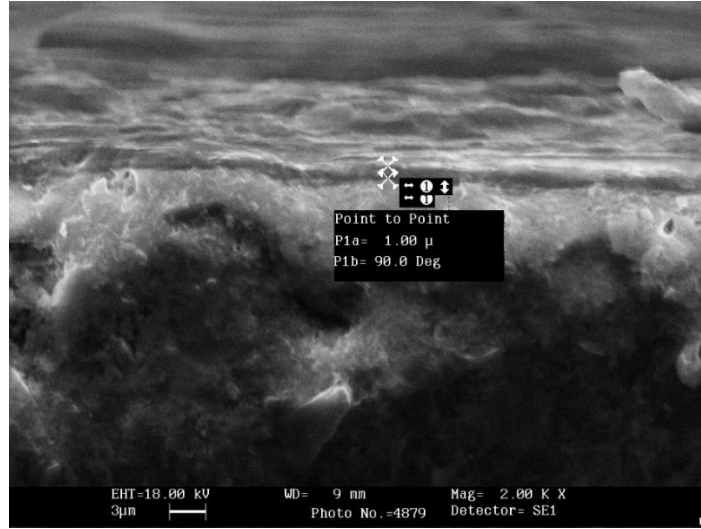


Figure 4. The cross-section of the alumina substrate coated with nanostructured tin oxide

In continuation, the results of the proposed gas chromatography sensor are obtained and its connection to the output reading circuit is examined. Firstly, the sensor reached a temperature of 250 °C by the heater. After the sensor response stabilized, certain concentrations of CO gas up to 470 PPM were injected into the chamber to obtain the sensitivity of the sensor's sensitive surface using equation (1) according to the other works [30, 31].

$$S = (Ra - Rg) / Rg = (Ig - Ia) / Ia \quad (1)$$

Resistance in ambient air is denoted by  $Ra$ , and resistance in the presence of the target gas is denoted by  $Rg$ . Similarly,  $Ig$  and  $Ia$  are the measured currents in the presence of the target gas and ambient air, respectively. The sensor resistance in the absence of the target gas (exposed to air) is 169 kΩ, and the output current measured is less than 3 nA. This is while in the test with a concentration of 470 ppm, the sensor resistance was measured to be 1.12 kΩ and the output current was 2.82 μA. Using the STM32F107VC microcontroller, the current was measured with a resolution of 805 μV using the proposed readout circuit. Considering the sensor's sensitivity of 6 nA/ppm and the feedback resistance ( $R_f$ ) of 500 kΩ, the output voltage per 1 PPM amounts to 3 mV, which falls within an acceptable range for a 12-bit ADC. Consequently, the minimum detection range is set at 1 PPM.

Figure 5.a illustrates the intrinsic sensitivity of the sensor proposed and developed in [19, 20] when exposed to CO gas. At low concentrations (0 to 100 PPM), the sensor demonstrates a notably steep slope of changes, indicating its high sensitivity. However, as the impurity concentration increases and the sensor tends toward saturation, the slope of the curve decreases. Consequently, the graph can be approximated with a bimodal function using a piecewise linear approximation. The results show that at a constant temperature of 250 °C, the sensor resistance varies in the range of 1.12 kΩ to 169 kΩ depending on the concentration of CO. It is clear that in the presence of CO gas, due to the release of free electrons, the sensor resistance has decreased and then saturated, while with the removal of the target gas, the resistance has increased and almost returned to its initial value.

The calculated response time and recovery time values for different gas concentrations are 27.527 seconds and 39 seconds, respectively, as shown in Figure 5.b. To study the stability of the sensor response, two experiments were conducted at the operating temperature of 250 °C, each lasting 56 hours, using pure N<sub>2</sub> gas and N<sub>2</sub> gas containing 1% CO. The stability of the sensor was observed in both cases. Additionally, the sensor sensitivity is 6 nA/ppm.

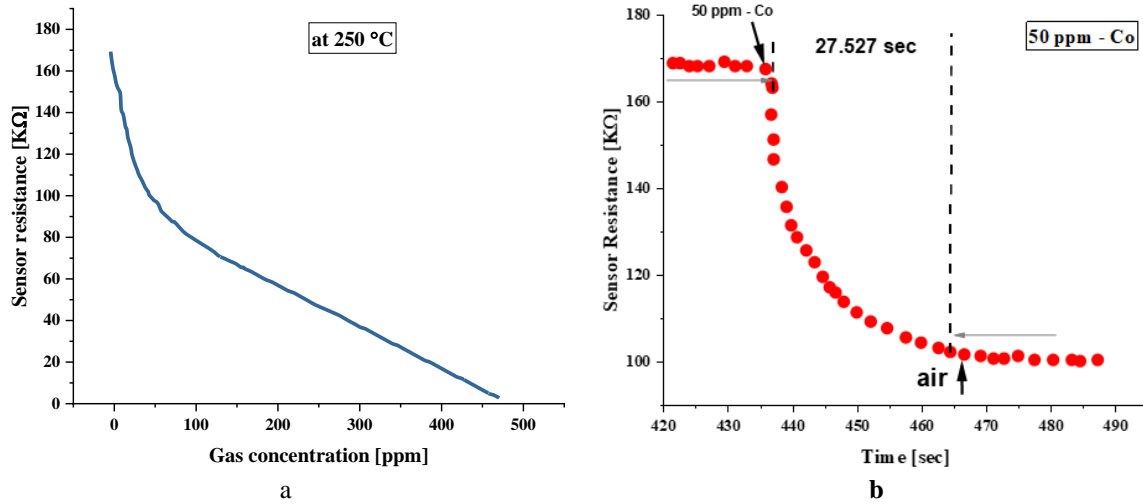


**Figure 5:** Sensor resistance a) Response to different concentrations of CO gas applied to the sensor. b) Response time for 50ppm of CO gas.

#### 4. Output Reading Circuit

This section discusses the AD623 Instrumentation Amplifier, a popular choice for such applications due to its ease of use, low power consumption, and high accuracy. The AD623 is an integrated single-supply instrumentation amplifier that allows for easy gain adjustment with a single external resistor. In our gas sensing circuit, the AD623 is configured to amplify the minute changes in resistance of the SnO<sub>2</sub> thin film, which varies in response to gas concentration. The high common-mode rejection ratio (CMRR) of the AD623 ensures that unwanted signals, such as noise from the environment or variations in the power supply, are significantly reduced, resulting in a cleaner and more accurate reading from the gas sensor. In the output reading circuit, the amplified signal from the AD623 is then fed into an analog-to-digital converter (ADC), translating the analog signal into a digital value that can be processed and read by a microcontroller. This setup allows for precise monitoring and analysis of gas concentrations, critical for applications in environmental monitoring, industrial safety, and health sectors. In conclusion, the AD623 instrumentation amplifier, with its precision amplification and ease of integration, significantly enhances the performance and reliability of the gas sensor system. By accurately amplifying the sensor's signal and ensuring that it is free from external noise and interference, the IA enables precise and reliable gas concentration measurements.

By changing the resistance of the sensor from 169 KΩ to 1.12 KΩ, the output voltage changes in the range of 720 mV to 2876 mV. Using a 12-bit ADC and an STM32F107VC microcontroller with a resolution of 0.805 μV, the output voltage was measured. Figure 6. shows the proposed deflection-type Wheatstone bridge circuit used to measure changes in the sensor resistance. The resistance R1 is used to adjust the sensitivity of the bridge, and R2 is the zero-adjustment resistor used for gas sensor calibration. The output voltage of the bridge varies proportionally with the change in the sensor layer conductivity and is connected to the AD623. The circuit is designed in such a way that the low-level bridge output is amplified and converted to a voltage that can be transferred to an ADC. AD623 is an IA that offers high-precision amplification of small signals. It has a high CMRR and a low input offset voltage, making it suitable for amplifying small differential signals in noisy environments. AD623 has the advantages of easy gain adjustment and a low loading effect. Figure 7. shows the illustration of the designed printed circuit board (PCB). The gain can be adjusted by changing the  $R_{Gain}$  resistor and can be calculated using the equation (2).

$$Gain = \frac{100 K\Omega}{R_{Gain}} + 1 \quad (2)$$

With  $R_{Gain}=100 K\Omega$ , the gain is obtained as 2. Using equation (3), the output voltage of the instrumentation amplifier can be calculated differentially.

$$v_o = Gain(v_2 - v_1) \quad (3)$$

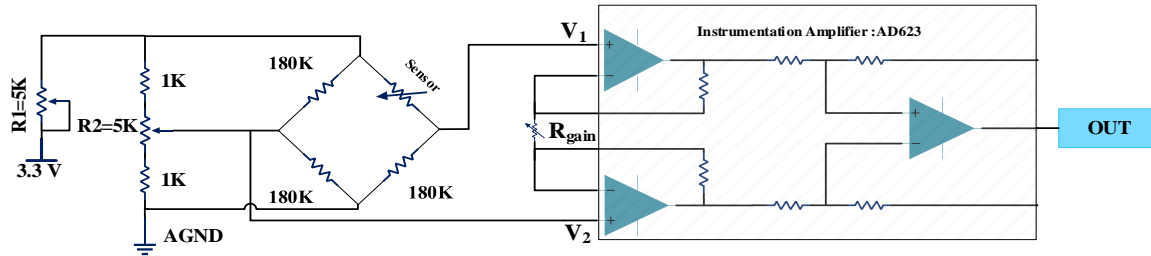


**Figure 6:** Proposed Circuit for readout and amplifying the output signal of the proposed sensor.

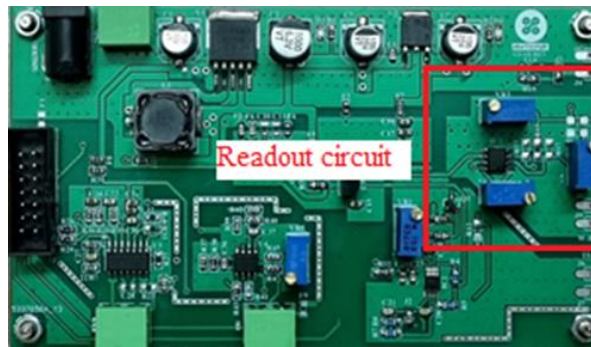


**Figure 7:** Illustration of the designed PCB.

## 5. Conclusions

This research attempts to investigate the challenges associated with the fabrication of nanocrystalline  $\text{SnO}_2$  thin films for use in carbon monoxide gas sensors along with the fabrication of an appropriate electronic circuit for the output reading so that the output has a suitable resolution, and at the same time, the effects of offset and amplifier noise should be negligible in the output voltage.

The sol-gel synthesis process has proven to be controllable in mitigating crack formation, thereby enhancing the structural integrity of the thin films on aluminum oxide ( $\text{Al}_2\text{O}_3$ ) substrates. The proposed gas sensor, characterized by its nanolayered structure, exhibited commendable sensitivity to varying concentrations of CO gas, as evidenced by the well-defined relationship between sensor resistance and gas concentration. The XRD analysis confirmed the successful formation of nanocrystalline tin oxide coatings on alumina substrates, with a calculated crystal size providing insights into the structural characteristics of the thin films. SEM images revealed a transformation in surface morphology, emphasizing the role of porosity in influencing gas sensor performance. The uniformity and distribution of the thin tin oxide layer, coupled with the presence of dispersed porous grains, contribute to an enhanced interaction between the sensor layer and the target analyte. The proposed gas sensor, integrated with a carefully designed output reading circuit,



demonstrated notable response and recovery times, essential parameters for real-world gas sensing applications. The stability of the sensor over an extended duration, observed during experiments with pure N<sub>2</sub> gas and N<sub>2</sub> gas containing 1% CO, underscores its reliability in diverse environmental conditions. This study, encompassing the synthesis methodology, structural analysis, and sensor performance evaluation, establishes a foundation for the development of effective and reliable CO gas sensors. The positive outcomes demonstrated that the sensor exhibits rapid response times of approximately 27.5 seconds and recovery times of about 39 seconds, with a minimum detection limit set at 1 PPM. Extended testing in environments of pure N<sub>2</sub> and 1% CO has confirmed the sensor's notable stability and reliability, marking a significant advancement in CO gas detection technology.

## References

- [1] Seiyama, Tetsuro, et al. "A new detector for gaseous components using semiconductive thin films." *Analytical Chemistry* 34.11 (1962): 1502-1503.
- [2] Liu, Jiancheng, et al. "BNQDs sensitized in-situ growth SnO<sub>2</sub> nanotube arrays for enhancing the gas sensing performances to isopropanol." *Colloids and Surfaces A: Physicochemical and Engineering Aspects* 690 (2024): 133828.
- [3] Si, Renjun, et al. "The stability of SnO<sub>2</sub> and In<sub>2</sub>O<sub>3</sub> gas sensors to water under temperature modulation mode." *Sensors and Actuators B: Chemical* 393 (2023): 134222.
- [4] Fan, Huiqing, et al. "Hydrothermal synthesis and their ethanol gas sensing performance of 3-dimensional hierarchical nano Pt/SnO<sub>2</sub>." *Journal of Alloys and Compounds* 909 (2022): 164693.
- [5] Selvam, Goban Kumar Panneer, María de la Luz Olvera Amador, and Arturo Maldonado Álvarez. "Gas sensing capabilities of sol-gel dip-coated pure SnO<sub>2</sub> thin films for CO and C<sub>3</sub>H<sub>8</sub> detection." *Journal of Materials Science: Materials in Electronics* 35.24 (2024): 1621.
- [6] Kong, Yulin, et al. "SnO<sub>2</sub> nanostructured materials used as gas sensors for the detection of hazardous and flammable gases: A review." *Nano Materials Science* 4.4 (2022): 339-350.
- [7] Xie, Renjie, Jianbin Lu, and Youqiang Liu. "Carbon monoxide gas sensing properties of SnO<sub>2</sub> modified metal-organic skeleton derived NiO." *Sensors and Actuators A: Physical* 367 (2024): 115038.
- [8] Simões, Agnes Nascimento, et al. "Room-temperature SnO<sub>2</sub>-based sensor with Pd-nanoparticles for real-time detection of CO dissolved gas in transformer oil." *Materials Chemistry and Physics* 311 (2024): 128576.
- [9] Suvarna, Thirukachhi, et al. "Investigation on Sb-doped SnO<sub>2</sub> as an efficient sensor for the detection of formaldehyde." *Materials Today Communications* 37 (2023): 107438.
- [10] Mendoza, Frank, et al. "Room temperature gas sensor based on tin dioxide-carbon nanotubes composite films." *Sensors and Actuators B: Chemical* 190 (2014): 227-233.
- [11] De Luca, L., et al. "Hydrogen sensing characteristics of Pt/TiO<sub>2</sub>/MWCNTs composites." *International journal of hydrogen energy* 37.2 (2012): 1842-1851.
- [12] Aroutiounian, V. M., et al. "Manufacturing and investigations of i-butane sensor made of SnO<sub>2</sub>/multiwall-carbon-nanotube nanocomposite." *Sensors and Actuators B: Chemical* 173 (2012): 890-896.
- [13] Van Hieu, Nguyen, et al. "Gas-sensing properties of tin oxide doped with metal oxides and carbon nanotubes: A competitive sensor for ethanol and liquid petroleum gas." *Sensors and Actuators B: Chemical* 144.2 (2010): 450-456.
- [14] Baranwal, Jaya, et al. "Electrochemical sensors and their applications: A review." *Chemosensors* 10.9 (2022): 363.
- [15] Perumalsamy, Revathy. "A CMOS switched capacitor filter based potentiometric readout circuit for chemfet sensor." Diss. 2018.
- [16] Aswal, Dinesh K., and Shiv K. Gupta. *Science and technology of chemiresistor gas sensors*. Nova Publishers, 2007.
- [17] Graf, Markus, et al. "CMOS monolithic metal-oxide sensor system comprising a microhotplate and associated circuitry." *IEEE Sensors Journal* 4.1 (2004): 9-16.

- [18] Cardinali, G. C., et al. "A smart sensor system for carbon monoxide detection." *Smart sensor interfaces* (1997): 113-134.
- [19] Asilian, Amirhosein, and S. Mohammadali Zanjani. "Design and fabrication of an amperometric CO gas sensor and a readout circuit using a low-noise trans-impedance amplifier to achieve standard analog outputs." *AEU-International Journal of Electronics and Communications* 171 (2023): 154864.
- [20] Asilian, Amirhosein, and S. Mohammadali Zanjani. "Application of Levenberg-Marquardt Backpropagation Algorithm in Artificial Neural Network for Self-Calibration of Deflection Type Wheatstone Bridge Circuit in CO Electrochemical Gas Sensor." *Majlesi Journal of Electrical Engineering* 18.1 (2024): 21-32.
- [21] Baroncini, M., et al. "A simple interface circuit for micromachined gas sensors." *Sensors and Actuators A: Physical* 109.1-2 (2003): 131-136.
- [22] Khakpour, Reza, M. N. Hamidon, and Guy Vandenbosch. "Design and fabrication of an auto calibration interface circuit for thick-film multi gas sensors." *Sensors and Actuators* 204 (2013): 48-57.
- [23] Futane, N. P., et al. "Nanocrystalline ZnO based MEMS gas sensors with CMOS ASIC for mining applications." *International Journal on Smart Sensing and Intelligent Systems* 1.2 (2008): 430-422.
- [24] Zanjani, Sayed Mohammad Ali, and Mostafa Parvizi. "Design and simulation of a bulk driven operational trans-conductance amplifier based on CNTFET technology." *Journal of Intelligent Procedures in Electrical Technology* 12.45 (2021): 65-76.
- [25] Jeng, Jiann-Shing. "The influence of annealing atmosphere on the material properties of sol-gel derived SnO<sub>2</sub>: Sb films before and after annealing." *Applied surface science* 258.16 (2012): 5981-5986.
- [26] Ferri, Giuseppe, et al. "Full range analog Wheatstone bridge- based automatic circuit for differential capacitance sensor evaluation." *International Journal of Circuit Theory and Applications* 45.12 (2017): 2149-2156.
- [27] Devesa, S., et al. "Williamson-hall analysis in estimation of crystallite size and lattice strain in Bi<sub>1-x</sub>Fe<sub>x</sub>O<sub>6</sub> prepared by the sol-gel method." *Materials Science and Engineering: B* 263 (2021): 114830.
- [28] Han, Tao, et al. "Carbon nanotubes and its gas-sensing applications: A review." *Sensors and Actuators A: Physical* 291 (2019): 107-143.
- [29] Beniwal, Ajay, and Vibhu Srivastava. "Sol-gel assisted nano-structured SnO<sub>2</sub> sensor for low concentration ammonia detection at room temperature." *Materials Research Express* 6.4 (2019): 046421.
- [30] Kadhim, Imad H., H. Abu Hassan, and Q. N. Abdullah. "Hydrogen gas sensor based on nanocrystalline SnO<sub>2</sub> thin film grown on bare Si substrates." *Nano-Micro Letters* 8 (2016): 20-28.
- [31] Lupan, Oleg, Lee Chow, and Guangyu Chai. "A single ZnO tetrapod-based sensor." *Sensors and Actuators B: Chemical* 141.2 (2009): 511-517.